2013

Blue luminescence and Zn acceptor in GaN

Denis Demchenko
Virginia Commonwealth University, ddemchenko@vcu.edu

Michael A. Reshchikov
Virginia Commonwealth University, mreshchi@vcu.edu

Demchenko, D.O. and Reshchikov, M.A. Blue luminescence and Zn acceptor in GaN. Physical Review B, 88, 115204 (2013).

Blue luminescence and Zn acceptor in GaN

D. O. Demchenko and M. A. Reshchikov
Department of Physics, Virginia Commonwealth University, Richmond, Virginia 23284, USA
(Received 24 June 2013; published 6 September 2013)

In this paper, we present a comparison of exchange-tuned hybrid density functional calculations with experimental data obtained for the Zn acceptor in GaN. Since this acceptor is one of the few reliably identified defects in GaN, we use Zn-doped GaN as a test case for the widely used HSE06 hybrid functional method of calculations of defect properties in semiconductors. Here, we present the experimental results of luminescence measurements in Zn-doped GaN from which we obtain Zn acceptor defect levels. They are compared with theoretically calculated defect thermodynamic and optical transition levels as well as the zero-phonon line associated with this acceptor. We also analyze the dependence of the results on the exchange-tuning procedure used in the HSE06 hybrid functional. Excellent agreement with the experiment is obtained when the amount of exact exchange in HSE06 is tuned to reproduce the GaN experimental band gap. This favorable comparison with the experimental results for a well-established defect suggests that the exchange-tuned HSE06 hybrid functional yields accurate defect properties in GaN and, therefore, has significant predictive power.

DOI: 10.1103/PhysRevB.88.115204 PACS number(s): 78.55.Cr, 61.72.uj, 71.15.Mb, 71.55.Eq

I. INTRODUCTION

Identification of point defects in semiconductors and their description with first-principles calculations is an important and challenging problem. Defects in GaN are of particular interest due to the wide use of this material in electronic and light-emission applications. Because of the technological importance, large amounts of experimental data have been accumulated with regard to the properties of defects in GaN. Nevertheless, point defects which may detrimentally affect device performance are still poorly understood. Theoretical calculations inevitably use certain assumptions and fitting parameters, but the use and applicability of such parameters to specific defects are not always justified or agreed upon. In addition, calculations of defect properties in semiconductors always involve a wide range of corrections, which are necessary to remove significant errors originating from several different sources. The exact application procedures for these corrections are still being debated. Another problem, impeding the progress in defect physics, is that reliable experimental data are not always available for comparison with theoretical results because very few defects with well-studied characteristics are reliably identified in GaN. One such defect that can be used as a test case for evaluating the applicability of theoretical methods is the Zn acceptor.

It is known that, in GaN, Zn substitutes for Ga and introduces an acceptor level at $E_A = 0.3$–0.4 eV above the top of the valence-band maximum (VBM).[1–4] This value is comparable to the Zn_{Ga} acceptor ionization energy (330–364 meV) calculated within the effective-mass approximation.[5,6] It is also established that the Zn_{Ga} defect is responsible for the blue luminescence (BL) band in Zn-doped GaN as well as in undoped GaN grown by metal-organic chemical-vapor deposition (MOCVD) or hydride vapor phase epitaxy (HVPE) techniques.[4] The BL band is caused by transitions from a shallow donor (at low temperatures) and from the conduction band (above 100 K) to the Zn_{Ga} acceptor. It has a luminescence peak at ~2.9 eV and a zero-phonon line at ~3.10 eV at 15 K.[4] In this paper, we compare the experimental results for the BL band with first-principles calculations based on the HSE06 hybrid functional,[7] which recently has become the preferred method for defect calculations in semiconductors.

II. EXPERIMENTAL RESULTS

We studied a number of GaN samples grown by HVPE and MOCVD techniques on *c*-plane sapphire substrates. These included an undoped GaN sample (No. th1011) with a concentration of Zn, N_{Zn}, less than 5×10^{15} cm^{-3} due to contamination during the HVPE growth, and several MOCVD-grown GaN samples heavily doped with Si ($N_{Si} = 10^{19}$cm^{-3}), which contained different concentrations of Zn ($N_{Zn} = 10^{14}$–10^{18} cm^{-3}). Photoluminescence (PL) spectra from all the samples exhibited the BL band with a maximum at about 2.9 eV.

The shape and position of the BL band can be best studied in a sample unintentionally doped with Zn (Fig. 1). For this sample, the BL band maximum is at 2.88 eV at 15 K, and the fine structure at the high-energy side of the band can be explained by electron-phonon coupling, involving two dominant phonon modes: the LO lattice mode with a phonon energy of 91 meV and a local mode with a phonon energy of 36 meV. The results obtained here are similar to the results on undoped and Zn-doped GaN reported in Refs. 8 and 9. A sharp peak at 3.087 eV is attributed to the zero-phonon line (ZPL). With increasing temperature from 15 to 50 K, the BL band shifts to higher energies by about 20 meV, and its fine structure becomes less resolved. This shift can be explained by an assumption that the donor-acceptor-pair (DAP) transitions at 15 K, involving a shallow donor and the Zn_{Ga} acceptor, are replaced with transitions from the conduction band to the same acceptor (eA transitions) above 50 K due to the thermal emission of electrons from the shallow donor to the conduction band. This assumption is supported by a characteristic transformation of the ultraviolet luminescence (UVL) band (Fig. 1). At 15 K, the UVL band consists of a main peak at 3.262 eV and its LO phonon replica at 3.170 eV, and both are attributed to DAP-type transitions from a shallow donor to an unidentified shallow acceptor in GaN. At 50 K,

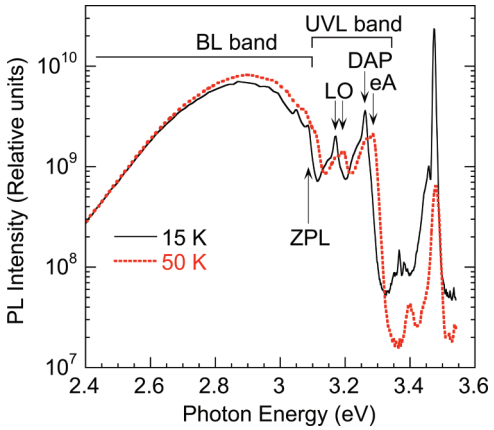

FIG. 1. (Color online) PL spectra of undoped GaN at 15 and 50 K.

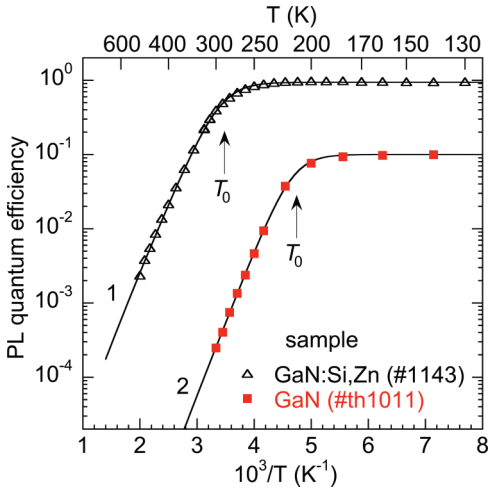

FIG. 2. (Color online) Temperature dependence of the quantum efficiency η for the BL band in undoped GaN (sample th1011) and Si-Zn co-doped GaN (1143). $P_{\rm exc} = 0.001$ W/cm^2. Lines are fit using Eq. (1) with the following parameters: $\eta_0 = 0.94$, $\tau_A = 5.5 \times 10^{-7}$ s, $E_A = 310$ meV, $C_{pA} = 7 \times 10^{-7}$ (for curve 1), $\eta_0 = 0.1$, $\tau_A = 5 \times 10^{-5}$ s, $E_A = 350$ meV, and $C_{pA} = 8 \times 10^{-7}$ (for curve 2).

these peaks become barely visible and give way to the eA peak at 3.285 eV and its LO phonon replica at 3.194 eV (Fig. 1).

The difference between positions of the eA and DAP peaks can be regarded as the effective ionization energy of the shallow donor ($E_D \approx 20$ meV). A peak at 3.475 eV is attributed to an exciton bound to a neutral shallow donor. The peak is shifted to higher energy by 4 meV from its position in thick strain-free GaN (3.471 eV).[4] From this, we conclude that the band gap in this sample is increased due to biaxial strain by 4 meV from the value in strain-free GaN (3.503 eV).[10] By taking into account the estimated band gap in our sample ($E_g = 3.507$ eV), the effective ionization energy of the shallow donor ($E_D = 20$ meV), and position of the ZPL ($E_0 = 3.087$ eV), we find the position of the acceptor level from the top of the valence band at 15 K as $E_A = E_g - E_0 - E_D = 0.400$ eV. It is interesting to note that, in Ref. 8, the same value of E_A has been obtained for another more strained GaN layer by using $E_0 = 3.098$ and $E_g = 3.518$ eV. Thus, accounting for the strain in the studied samples and the effective energy of the shallow donor, we conclude that, in strain-free GaN, the optical transitions from the conduction band to the Zn_{Ga} acceptor with $E_A = 0.40$ eV (eA transitions) have the ZPL at 3.10 eV and the band maximum at 2.90 eV.

The value of E_A at higher temperatures can also be estimated from the thermal quenching of PL. In n-type GaN, the BL band is quenched at temperatures above 200 K with the slope of the Arrhenius plot corresponding to 0.35 eV. Figure 2 shows typical temperature dependencies for the BL quantum efficiency in two characteristic samples. In the undoped GaN, a transition from the temperature-independent region to the quenching region occurs at a characteristic temperature of $T_0 = 210$ K, whereas, in GaN co-doped with Si and Zn, $T_0 = 290$ K. The PL quantum efficiency η, defined as a ratio of the PL intensity $I^{\rm PL}$ to the electron-hole pair generation rate G has the following temperature dependence for n-type semiconductors:[11,12]

$$\eta(T) \frac{\eta_0}{1 + (1 - \eta_0)\,\tau_A C_{pA} g^{-1} N_v \exp\left(-\frac{E_A}{kT}\right)}. \qquad (1)$$

Here, η_0 is the quantum efficiency of the BL band at $T < T_0$ where the BL intensity is temperature independent, τ_A is the PL lifetime for the BL band determined from the time-resolved PL measurements, C_{pA} is the hole-capture coefficient for the Zn_{Ga} acceptor, g is its degeneracy factor ($g = 2$), N_v is the effective density of states in the valence band, and k is Boltzmann's constant. The values of η_0 were estimated from the analysis of temperature dependencies of other PL bands in these samples (similar to the analysis conducted in Ref. 12) and independently from comparison of the integrated PL intensity of the BL band with intensities of PL bands in calibrated samples. The values of C_{pA} and E_A, obtained from the best fit and given in the caption for Fig. 2, are very close to previously reported values.[4,11–14] The value of E_A (about 350 meV) is slightly lower than the value at 15 K (400 meV), possibly due to a small decrease in the acceptor ionization energy with increasing temperature from 15 to 200–300 K. In samples with a high concentration of Si and Zn, such as the degenerate Si-Zn co-doped sample No. 1143, E_A is lower than 350 meV because of the band-gap shrinkage and the broadening of the acceptor level.

In contrast to the data presented above for conductive n-type GaN (undoped or Si-Zn co-doped), in high-resistivity or p-type GaN doped with Zn, the thermal quenching of the BL band is very abrupt (not shown here), the slope of the quenching corresponds to the activation energy of about 1.0 eV, and the characteristic temperature of the quenching shifts to higher temperatures with increasing excitation intensity.[13,14] This unusual behavior of the BL band was explained by a sudden redirection of the recombination flow from the Zn_{Ga} acceptor to an unknown nonradiative defect with increasing temperature at some critical value T^*, which increased with excitation intensity.[13] Remarkably, the ionization energy of the Zn_{Ga} acceptor could be determined from the shift in T^* with excitation intensity, and the value obtained for high-resistivity or p-type GaN:Zn samples ($E_A = 340-350$ meV) agrees very well with the values of E_A obtained from the quenching of the BL band in conductive n-type GaN.

III. METHODS OF CALCULATIONS

Our calculations are based on the Heyd-Scuseria-Ernzerhof (HSE) hybrid functional[7] as implemented in the Vienna *ab initio* simulation package program.[15] We use the HSE hybrid functional with the fraction of exact exchange of 0.312 and the screening parameter of 0.2 $Å^{-1}$. These parameters accurately reproduce both the band gap and the lattice properties of bulk GaN.[16] The resulting band gap of 3.5 eV is in good agreement with the low-temperature experimental value of 3.50 eV.[10,17] Computed relaxed lattice parameters for wurtzite GaN ($a = 3.210$ Å, $c = 5.198$ Å, and $u = 0.377$) also agree with experimental values ($a = 3.189$ and $c = 5.185$ Å).[18] The 128 atom supercells were used with atomic structures relaxed using HSE hybrid functional calculations to yield forces of 0.05 eV/Å or less. We tested supercells containing up to 300 atoms and found 128 atom cells to be sufficient. The plane-wave basis sets with a 400-eV cutoff at the Γ point were used in all the electronic structure calculations. In the 128 atom supercells, the use of a $2 \times 2 \times 2$ mesh as opposed to Γ-point only eigenvalues resulted in errors less then 0.05 eV. Spin-polarized calculations were performed in all cases. Details on the systematic tests, performed in order to evaluate possible sources and values of errors for defects in GaN, are published elsewhere.[19]

The defect formation energy quantifies the probability of a lattice defect to be realized. It is defined as the total energy difference of the supercell with the defect E_d and the bulk supercell E_{bulk} adding (or subtracting) the chemical potentials of the missing (added) atoms in the defect cell μ_i and adding the charging energy of a defect qE_F for nonzero charge states. The chemical potentials for Zn, N, and Ga are taken from HSE calculations of the metallic Zn, a N_2 molecule, and metallic Ga, respectively. For charged defects, the use of periodic boundary conditions leads to unphysical electrostatic interactions between the defect periodic images and the compensating background charge density, which is added to keep the calculation charge neutral. The proper application of the corrections of various physical origins has been analyzed in literature in great detail.[20] Here, following Lany and Zunger,[20] we use Makov and Payne[21,22] corrections for spurious electrostatic interactions up to third order for charged defects.

IV. DISCUSSION

A. Formation energies and thermodynamic transition levels

Figure 3 shows the formation energies of the Zn_{Ga} substitutional defect. From our calculations, it is evident that Zn_{Ga} is an acceptor with the $0/-$ thermodynamic transition level at 0.45 eV above the VBM. The two panels show the formation energies computed for Ga-rich and Ga-poor growth conditions, which differ by the GaN enthalpy of formation (computed here to be −1.25 eV) in the definition of Ga and N chemical potentials. Depending on the growth conditions, the probability of the Zn_{Ga} acceptor formation changes with Ga-poor growth being more favorable for incorporating Zn acceptors into the GaN lattice. In *n*-type GaN, the Zn_{Ga} acceptor would provide a compensating effect and is, therefore, always energy efficient with formation energy being negative for Ga-poor growth

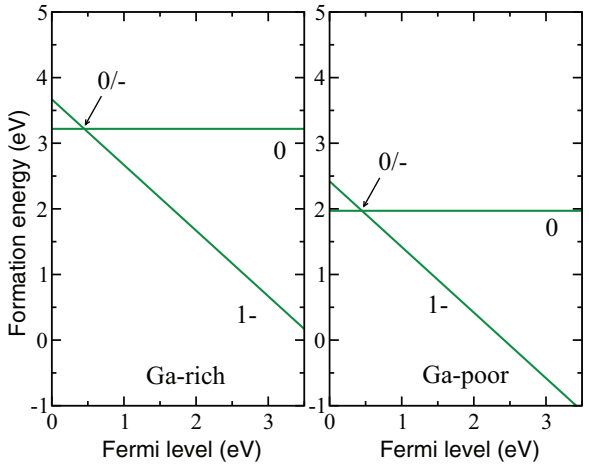

FIG. 3. (Color online) Calculated formation energies of Zn_{Ga} as a function of the Fermi energy in the band gap of GaN in Ga-rich and Ga-poor growth conditions. The zero of the abscissa corresponds to the valence-band maximum, and the conduction-band minimum (CBM) is at 3.5 eV. Charge states are indicated for each line. The computed $0/-$ thermodynamic transition level for the Zn_{Ga} acceptor is at 0.45 eV.

regime. This finding is consistent with the high intensity of the BL band in unintentionally doped *n*-type GaN.[4]

B. Optical transition levels

Transitions involving the Zn_{Ga} acceptor are shown in Fig. 4(a), which depicts a configuration coordinate diagram for the two charge states of the Zn_{Ga} acceptor. Optical transitions are shown with vertical arrows, and transitions that involve the emission of multiple phonons are shown with curved arrows. Initially, the lowest-energy charge state of the Zn_{Ga} acceptor in *n*-type GaN is negative (Fig. 3), shown by the lower curve labeled Zn_{Ga}^{-}. The absorption energy associated with this defect is 3.12 eV. However, we are not aware of any experimental data for the PL excitation spectra associated with the BL band. The BL band is commonly excited with a band-to-band transition [shown with a vertical arrow with the length equal to the GaN band gap (3.50 eV)]. Upon band-edge absorption of a photon, an electron-hole pair is created, and the negatively charged Zn_{Ga} acceptor captures the free hole (transition schematically shown with a curved arrow from the $Zn_{Ga}^{-} + e^{-}$ state to $Zn_{Ga}^{0} + e^{-}$, where e^{-} indicates an electron in the conduction band). Upon relaxation into its lowest-energy geometry, the electron in the conduction band recombines with the hole localized on the Zn_{Ga} center producing a luminescence peak with photon energy of 2.94 eV, returning the Zn_{Ga} acceptor into its lowest-energy charge state. Thus, the exchange-tuned HSE06 hybrid functional calculated value of the optical transition energy is in excellent agreement with the measured BL peak of 2.90 eV.

Although the Zn_{Ga} acceptor creates a relatively deep level at 0.45 eV, the electronic wave function of the defect state is weakly localized. In contrast to the results obtained for the Mg acceptor in GaN,[16] following atomic relaxation we do not find the localized state for a Zn acceptor. Figure 4(b) shows the charge density of the hole captured on the Zn_{Ga}

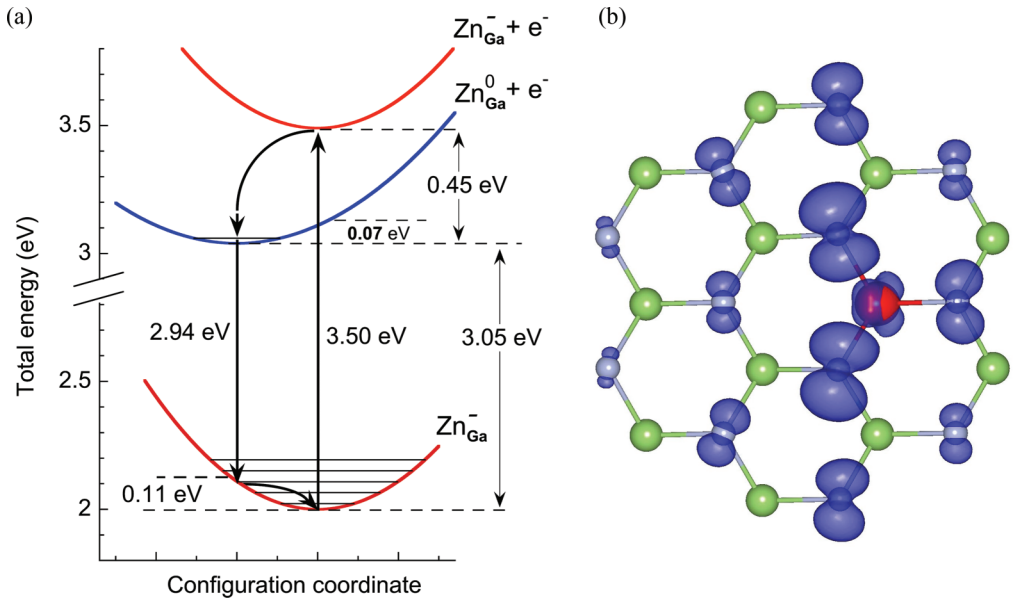

FIG. 4. (Color online) (a) Calculated optical transitions via the Zn_{Ga} acceptor. The configuration coordinate diagram shows relatively small lattice distortions. The emission energy of 2.94 eV corresponds to electronic transition from the conduction band to neutral Zn_{Ga}^{0}, returning the acceptor to a negative charge state Zn_{Ga}^{-}. This transition is in good agreement with the measured BL maximum of 2.90 eV. The energy separation between two minima (3.05 eV) agrees well with the zero-phonon line for the BL band (3.10 eV). (b) Calculated charge density of the hole trapped on the Zn_{Ga}^{0} acceptor is plotted in the [0001] plane for clarity. The isosurfaces are plotted at 6% of the maximum value. The hole wave function is weakly localized around the Zn atom (large red sphere), having significant density on nitrogen (small gray spheres) well beyond the second-nearest neighbors.

acceptor after the photon absorption. The hole wave function is relatively spread out around the Zn atom and has a significant charge density on the nitrogen atoms, well beyond the second- and third-nearest neighbors. As a consequence of the weak localization, lattice distortions around the defect are modest. Nitrogen atoms relax outward from the Zn impurity by ∼3.4% of the bond length in the 1− charge state and by ∼3.5% in the neutral charge state. This leads to a relatively small value in the calculated Franck-Condon shift of 0.11 eV. The resulting zero-phonon energy is 3.05 eV, which is in excellent agreement with the measured ZPL of 3.10 eV. Finally, the Stokes shift is calculated to be 0.18 eV.

C. Accuracy of transition energies for hybrid functionals

In the HSE06 hybrid functional, the exchange interactions are split into long- and short-range parts with a screening parameter controlling this splitting range. The long-range exchange and all electronic correlations are computed with the Perdew-Burke-Ernzerhof[23] (PBE) theory of the generalized gradient approximation (GGA) to the density functional theory. The energy of short-range exchange interactions is computed as a mixture of a fraction α of exact Fock exchange and a fraction $(1-\alpha)$ of PBE exchange. The original HSE06 functional has been developed with $\alpha = 0.25$, which, as a rule, greatly improves the computed band gaps in most semiconductors.[24] However, in electronic structure calculations, and especially those related to defects in semiconductors, the remaining errors in the band gap can lead to significant errors in the defect formation energies and optical transitions. Therefore, it has become a common practice to tune the amount of the exact exchange α in the calculation to obtain a band-gap value in agreement with the experiment. In this paper, the results presented above are also computed using the HSE06 hybrid functional with the fraction of Fock exchange equal to 0.312, tuned to reproduce the experimental band gap in GaN.

As shown above, the theoretical results obtained with such a tuned HSE06 hybrid functional are in excellent agreement with presented experimental data for a well-understood defect in GaN, such as the Zn_{Ga} acceptor. However, it is important to estimate the accuracy of these calculations with respect to the tuning of exact exchange. We have performed the optical and thermodynamic transition energy calculations for different fractions of exact exchange within HSE06, ranging from GGA (zero fraction of exact exchange) to 0.312 while keeping the screening parameter constant and equal to 0.2 Å^{-1}. The results of these calculations are presented in Fig. 5, showing the evolution of the optical and thermodynamic transition levels with the increasing exact exchange fraction. Here, the optical transition level is defined as the transition level, corresponding to the maximum of emission, in order to emphasize the influence of the exact exchange fraction on the defect luminescence. Alternatively, the optical level could be defined as that corresponding to the zero-phonon line. However, since the zero-phonon line can be thought of as the band gap minus the thermodynamic transition level, it would be equivalent to tracking the latter. For all values of α, absorption and emission lines were computed according to the diagram in Fig. 4, using the formation energies obtained at different values of α. The experimental band gap for the energy of the electron in the conduction band was used in all optical level calculations, whereas, the thermodynamic level is calculated directly from the formation energies.

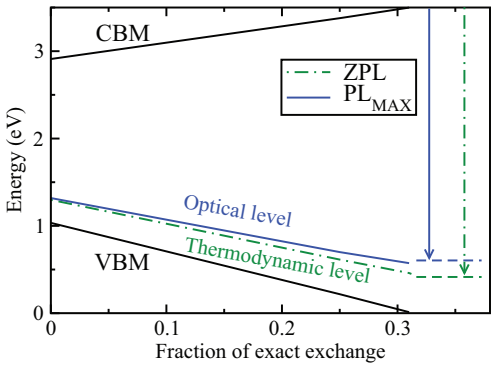

FIG. 5. (Color online) Calculated dependence of thermodynamic and optical transition levels on the fraction of exact exchange in HSE06 for the Zn_{Ga} acceptor. The thermodynamic transition level (green dashed-dotted line) is slightly lower than the optical transition level (blue solid line). The horizontal dashed lines in the lower right corner represent experimental values of transition levels. Vertical arrows show transitions corresponding to the experimental luminescence maximum (PL_{MAX}) and the ZPL.

The changes in positions of the VBM and the CBM are shown as the band gap increases linearly from 1.88 eV in the GGA limit to 3.50 for $\alpha = 0.312$. When the value of the experimental band gap is reached at $\alpha = 0.312$, the valence band is shifted down by 1.03 eV, whereas, the conduction band is moved up by 0.59 eV. The GGA computed thermodynamic and optical transition levels practically coincide, but they are both underestimated with values of 0.26 and 0.28 eV, respectively (relative to the VBM at $\alpha = 0$ in Fig. 5). With the increased fraction of exact exchange, both the thermodynamic and the optical transition levels tend to follow the valence band with slightly different lags. The difference between these two levels increases, reaching 0.11 eV for $\alpha = 0.312$ at the experimental band gap. For this fraction of exact exchange, the transition levels are approaching their corresponding experimental values to within 0.05 eV. For $\alpha = 0.312$, the calculated thermodynamic transition level is at 0.45 eV, and the optical level is at 0.56 eV above the VBM. This upward shift in the transition levels above the VBM is obtained without any postprocessing corrections to the host band gap.

The behavior of transition levels as a function of α shown in Fig. 5 suggests that the amount of exact exchange tuned to reproduce the host band gap also accurately reproduces defect-related electronic and optical properties. Although there are still unphysical interactions present in the calculations, mainly due to the use of periodic boundary conditions, the well-documented methods of correcting the resulting energies[20] remove the related errors. The problems related to the electronic exchange and correlations, present in the GGA treatments of the impurity problem, appear to be circumvented in the exchange-tuned HSE06 hybrid functional. Nevertheless, the remaining inaccuracies in band-structure calculations using HSE06 might still introduce errors to the defect formation energy calculations. In ZnO, for example, tuning of the band gap to the experimental value leads to an excessive downshift of the VBM with respect to the underlying d band.[25] This occurs since HSE06 results in an overestimated Zn d-band energy and a relatively large value of α is needed to compensate for the p-d band repulsion. In addition, previous hybrid functional studies of intrinsic defects in ZnO indicated that reproducing the experimental band gap might not guarantee the correct defect formation energies and transition levels,[26] even though one might expect an error in the underlying band structure of the host material to cancel in the calculation of the defect formation energy. Therefore, further studies are necessary to test the accuracy of this approach in materials with occupied d states. Nevertheless, the presented comparison of the results obtained with HSE06 and experimental data shows that this method can accurately predict electronic and optical properties of defects in materials where reproducing accurate d-band energies is not critical.

V. CONCLUSIONS

We have performed a detailed comparison of hybrid functional calculations of electronic and optical properties of Zn_{Ga} defects in GaN with experimental PL measurements. Overall, we find that the defect-related properties of the Zn_{Ga} acceptor in GaN, obtained with the exchange-tuned HSE06 hybrid functional, are in very good agreement with experimental values. The computed formation energies of the Zn_{Ga} acceptor produce the thermodynamic transition level of 0.45 eV above the valence-band maximum, which agrees with the value of 0.40 eV deduced from low-temperature PL spectra. We find that the measured PL spectra of the BL band in GaN, which is believed to be caused by the transitions via the Zn_{Ga} acceptor, are in excellent agreement with the calculated results. The computed maximum of the blue band is at 2.94 eV, whereas, the measured value is 2.90 eV. The zero-phonon line is computed to be 3.05 eV, which is also in agreement with the measured 3.10 eV. Since Zn_{Ga} is one of the few well-identified impurities in GaN, we also investigate the applicability of this theoretical approach for various fractions of exact exchange in the HSE06 hybrid functional, ranging from the GGA approximation to the fractions reproducing the experimental GaN band gap. We show that the commonly used tuning of the exact exchange to accurately reproduce the band gap of a particular host semiconductor produces reliable results.

ACKNOWLEDGMENTS

This work used the computational facilities of the VCU Center for High Performance Computing. The authors are grateful to A. Bakin from TUBS (Braunschweig, Germany) and D. C. Look (Wright State University) for providing the GaN samples used in this paper.

[1]B. Monemar, H. P. Gislason, and O. Lagerstedt, J. Appl. Phys. **51**, 640 (1980).
[2]M. Ilegems, R. Dingle, and R. A. Logan, J. Appl. Phys. **43**, 3797 (1972).
[3]J. I. Pankove, J. E. Berkeyheiser, and E. A. Miller, J. Appl. Phys. **45**, 1280 (1974).
[4]M. A. Reshchikov and H. Morkoç, J. Appl. Phys. **97**, 061301 (2005).

[5]F. Mireles and S. E. Ulloa, Phys. Rev. B **58**, 3879 (1998).
[6]H. Wang and A.-B. Chen, Phys. Rev. B **63**, 125212 (2001).
[7]J. Heyd, G. E. Scuseria, and M. Ernzerhof, J. Chem. Phys. **118**, 8207 (2003).
[8]M. A. Reshchikov, F. Shahedipour, R. Y. Korotkov, M. P. Ulmer, and B. W. Wessels, J. Appl. Phys. **87**, 3351 (2000).
[9]M. A. Reshchikov, H. Morkoç, R. J. Molnar, D. Tsvetkov, and V. Dmitriev, in *Blue Luminescence in Undoped and Zn-Doped GaN*, edited by Y. Arakawa, A. Rizzi, J. S. Speck, C. M. Wetzel, and E. T. Yu, MRS Symposia Proceedings No. 743 (Materials Research Society, Warrendale, PA, 2003), p. L11.1.
[10]B. Monemar, Phys. Rev. B **10**, 676 (1974).
[11]M. A. Reshchikov and R. Y. Korotkov, Phys. Rev. B **64**, 115205 (2001).
[12]M. A. Reshchikov, M. A. Foussekis, J. D. McNamara, A. Behrends, A. Bakin, and A. Waag, J. Appl. Phys. **111**, 073106 (2012).
[13]M. A. Reshchikov, A. A. Kvasov, M. F. Bishop, T. McMullen, A. Usikov, V. Soukhoveev, and V. A. Dmitriev, Phys. Rev. B **84**, 075212 (2011).
[14]M. A. Reshchikov, Phys. Rev. B **85**, 245203 (2012).
[15]G. Kresse and J. Furthmüller, Phys. Rev. B **54**, 11169 (1996).
[16]J. L. Lyons, A. Janotti, and C. G. Van de Walle, Phys. Rev. Lett. **108**, 156403 (2012).
[17]R. Dingle, D. D. Sell, S. E. Stokowski, and M. Ilegems, Phys. Rev. B **4**, 1211 (1971).
[18]H. Morkoç, *Handbook of Nitride Semiconductors and Devices* (Wiley, New York, 2008), Vols. 1–3.
[19]D. O. Demchenko, I. C. Diallo, and M. A. Reshchikov, Phys. Rev. Lett. **110**, 087404 (2013).
[20]S. Lany and A. Zunger, Phys. Rev. B **78**, 235104 (2008).
[21]G. Makov and M. C. Payne, Phys. Rev. B **51**, 4014 (1995).
[22]M. Leslie and M. J. Gillan, J. Phys. C **18**, 973 (1985).
[23]J. P. Perdew, K. Burke, and M. Ernzerhof, Phys. Rev. Lett. **77**, 3865 (1996).
[24]M. Marsman, J. Paier, A. Stroppa, and G. Kresse, J. Phys.: Condens. Matter **20**, 064201 (2008).
[25]L. Y. Lim, S. Lany, Y. J. Chang, E. Rotenberg, A. Zunger, and M. F. Toney, Phys. Rev. B **86**, 235113 (2012).
[26]S. J. Clark, J. Robertson, S. Lany, and A. Zunger, Phys. Rev. B **81**, 115311 (2010).